Metrol. Meas. Syst., Vol. 31 (2024), No. 4
DOI: 10.24425/mms.2024.150294

METROLOGY AND MEASUREMENT SYSTEMS
Index 330930, ISSN 0860-8229
www.metrology.wat.edu.pl

POWER-OF-SINE WINDOWS AS GENERALIZED MAXIMUM SIDELOBE DECAY WINDOWS – THEORY AND PROPERTIES: A REVIEW AND NEW RESULTS

Józef Borkowski, Adam Matusiak

Wroclaw University of Science and Technology, Faculty of Electronics, Photonics and Microsystems, Chair of Electronic and Photonic Metrology, Bolesława Prusa 53/55, 50-317 Wrocław, Poland (✉ *jozef.borkowski@pwr.edu.pl*)

Abstract

The paper presents the theoretical properties of power-of-sine time windows, including the property of maximum sidelobe decay. This family of windows is a generalisation of the widely known Maximum Sidelobe Decay (MSD) windows and is referred to as Generalised Maximum Sidelobe Decay (GMSD) windows. GMSD windows are used in methods such as DFT spectrum interpolation (IpDFT), due to their desirable properties for such applications. The paper presents the key results, including the analytical form of the frequency characteristics of GMSD windows and some of their properties. The formulas derived are useful for describing these properties.

Keywords: time windows, spectrum leakage, MSD, GMSD, power-of-sine windows.

1. Introduction

One of the most well-known methods for calculating the spectrum of a signal is the use of the FFT algorithm on a signal that has been modified by a measurement window, resulting in a *Discrete Fourier Transform* (DFT) not of the signal itself, but of the signal multiplied by a time window function. The main problem in using such a calculated spectrum are two adverse effects:

– spectrum leakage, which is the result of the convolution of the signal's spectrum and the spectrum of the time window (due to the multiplication of the signal by the window function in the time domain),
– the discrete nature of the obtained DFT spectrum, because the DFT transform determines the spectrum values only for N points of one period of the spectrum; this results in the computational resolution of the DFT (*i.e.* the frequency axis distance between consecutive DFT spectrum points) being too small for many applications.

The detrimental effects of spectrum leakage are reduced by using time windows other than rectangular [1]–[7]. The negative effects of the discrete nature of the spectrum can be reduced by using nonparametric and parametric methods of DFT spectrum interpolation [8]–[18].

This paper is dedicated to the first of the mentioned issues, *i.e.* the use of non-rectangular time windows, specifically the family of *Generalised Maximum Sidelobe Decay* (GMSD) windows, which includes one of the most popular and versatile time windows, the Hann (Hanning) window. Due to its properties, the GMSD window family has its particular applications, which will be the subject of a subsequent research on GMSD windows.

The GMSD time windows have their origins in the paper [1], where Rife and Vincent demonstrated that windows based on a cosine base exhibit the property of maximum sidelobe decay, provided that a specific condition on the coefficients a_h of the time window function's cosine series expansion is met. Additionally, the first practical analytical formula for the *Discrete-time Fourier Transform* (DtFT) of such windows was derived in [1], along with its

Article history: received April 29, 2024; revised June 9, 2024; accepted June 30, 2024; available online September 12, 2024.

application to frequency and amplitude estimation of a single tone in the spectrum. Since then, this family of windows has been referred to as the Rife-Vincent class I family, and over time also as *Maximum Sidelobe Decay* (MSD) windows, and less frequently, binomial windows. Another significant result regarding cosine-based windows was Nuttall's determination [3] of two conditions that the a_h coefficients must meet to achieve the maximum sidelobe decay condition. Belega in [7] found relations for the a_h coefficients based on Newton's binomial, which are a slightly improved version of the Rife and Vincent result from [1]. Besides meeting Nuttall's two conditions, the result from [7] also fulfills the window normalization condition according to which the maximum (central) value of the window function is equal to 1 (a condition not met by the Rife and Vincent version from [1]). Meanwhile, Borkowski *et al.* showed in [12] how to obtain the a_h coefficients meeting the window normalization condition directly from Rife and Vincent's result. Duda *et al.* in [13] indicated that MSD windows are identical to $\sin^p$ windows for even p. Borkowski *et al.* demonstrated in [14] that $\sin^p$ windows for odd p are identical to sine-based windows with b_h coefficients selected to ensure maximum sidelobe decay, which allowed the introduction of the term *Generalized Maximum Sidelobe Decay* (GMSD) for $\sin^p$ windows for all values of p (both even and odd) [14]. In this way, the GMSD time window family includes, as its subfamily, the MSD windows. Moreover, operating with a single parameter p instead of a set of a_h coefficient values is much more convenient when using this window in practice. In particular cases: for $p = 0$, the GMSD window takes the form of the rectangular window, and for $p = 2$, the form of the Hann window (often called the Hanning window).

The structure of the paper is as follows: after a mathematical introduction (Sect. 2), various definitions of GMSD windows are presented (Sect. 3), along with a complete proof of the maximum sidelobe decay property (Sect. 4, 5). Subsequently, the basic properties of GMSD windows are presented (Sect. 6, 7), which are useful in various applications.

2. Fourier analysis, time data window, DtFT, DFT – basic mathematical notations

Consider two cases of the signal $x(t)$. If $x(t)$ is a periodic signal with period T_x, it can be represented in the form of a complex Fourier series:

$$x(t) = \sum_{k=-\infty}^{+\infty} c_k e^{j2\pi kt/T_x}, \tag{1}$$

where the coefficients c_k form the discrete spectrum of the signal $x(t)$ for integer k:

$$c_k = \frac{1}{T_x}\int_{t_1}^{t_1+T_x} x(t)e^{-j2\pi kt/T_x}dt. \tag{2}$$

However, if $x(t)$ is a non-periodic signal for which a Fourier transform $F(f)$ exists, then $x(t)$ can be represented in the form:

$$x(t) = \int_{-\infty}^{+\infty} F(f)e^{j2\pi ft}df, \tag{3}$$

where the continuous spectrum $F(f)$ of the signal $x(t)$ is given by:

$$F(f) = \int_{-\infty}^{+\infty} x(t)e^{-j2\pi ft}dt. \tag{4}$$

In a practical DSP system, the spectrum is computed using N samples of the discrete signal $x_n = x(nT)$ (where $n = 0, 1, \ldots, N-1$) obtained from an A/D converter in the sampling process with a sampling rate $f_s = 1/T$. Then, both the relation (2) for periodic signals and the relation (4) for non-periodic signals can be approximated by the *Discrete-time Fourier Transform* (DtFT), which defines the continuous spectrum $X(f)$ of the discrete signal x_n multiplied by a time window w_n, which has nonzero values for $n \in [0, N-1]$ (in the simplest case $w_n = 1$ for the

rectangular window) and zero values for $n \notin [0, N-1]$:

$$X_\lambda = X(f = \frac{\lambda}{NT}) = \sum_{n=0}^{N-1} w_n x_n e^{-j2\pi n\lambda/N}. \tag{5}$$

The normalized frequency $\lambda = f \cdot NT = N f / f_s$ introduced in (5) is expressed in bin units and directly determines how many periods of the sinusoidal component with frequency f in Hz fit into the measurement window with a duration of NT. In moving from (2) to (5), the division by T_x is omitted, as T_x is often unknown.

The *Discrete Fourier Transform* (DFT) is defined as samples of the DtFT for $\lambda = k = 0, 1, \ldots, N-1$:

$$X_k = \sum_{n=0}^{N-1} w_n x_n e^{-j2\pi nk/N}. \tag{6}$$

The set of values $\{X_0, X_1, \ldots, X_{N-1}\}$ is most commonly computed using the FFT algorithm from the set $\{w_0x_0, w_1x_1, \ldots, w_{N-1}x_{N-1}\}$, *i.e.* the discrete signal x_n multiplied by the time window w_n. In low-cost DSP systems, selected spectrum points can also be calculated using the Goertzel algorithm instead of the FFT algorithm [17].

The spectra of DtFT and DFT defined by (5) and (6) allow for the estimation of the spectrum for both periodic and non-periodic signals. The DFT spectrum has all the features of the DtFT spectrum (including being periodic with a period of f_s on the frequency axis and being affected by the detrimental effect of spectrum leakage), and additionally possesses a discrete character, as it is determined only for integral values of k. This means that the computational resolution of the DFT, *i.e.* the spacing on the frequency axis between two adjacent DFT spectrum points, is 1 bin on the normalized frequency axis λ, or equivalently $f_s / N = 1/(NT)$ Hz on the frequency axis in Hz. If the computational resolution of the DFT is insufficient, it can be improved by computing (5) for non-integer values of λ (*i.e.* (6) for non-integer k). The only cost of such an improvement in DFT computational resolution is increased computation time. The computational resolution of the DFT should not be confused with the Fourier resolution defined by the main lobe width of the rectangular window, which also equals the inverse of the measurement window duration, thus 1 bin on the normalized frequency axis (1/(NT) Hz on the frequency axis in Hz). Fourier resolution can only be improved by increasing the duration of the measurement window, *i.e.* the measurement time of the signal.

The DtFT spectrum (5) represents the spectrum of the signal after being multiplied by the window function in the time domain. Consequently, it can be described as the convolution $F(\lambda) \otimes W(\lambda)$, where $F(\lambda)$ is the spectrum of the original signal in time and $W(\lambda)$ is the spectrum of the applied time window:

$$W(\lambda) = \sum_{n=0}^{N-1} w_n e^{-j2\pi n\lambda/N}. \tag{7}$$

The characteristic $W(\lambda)$, *i.e.* the DtFT of the applied time window, allows for the determination of a series of important properties of such a window, especially in relation to the rectangular window, which is often the reference window due to its well-known properties. The spectrum of the rectangular window is obtained from (7) by setting $w_n = 1$ and using the formula for the sum of a geometric series. The obtained spectrum $W(\lambda)$ of the rectangular window, denoted here as $D_N(\lambda)$, is known as the Dirichlet kernel of an N-point DtFT:

$$D_N(\lambda) = \sum_{n=0}^{N-1} e^{-j2\pi n\lambda/N} = e^{-\mathrm{j}\pi\lambda(N-1)/N} \frac{sin(\pi\lambda)}{sin(\pi\lambda/N)}. \tag{8}$$

In Section 4, the following approximation of (8) is used for small $\lambda \ll N$ and $N \gg 1$:

$$\frac{1}{N} D_N(\lambda) \approx e^{-\mathrm{j}\pi\lambda} \frac{sin(\pi\lambda)}{\pi\lambda} = e^{-\mathrm{j}\pi\lambda}\mathrm{sinc}(\lambda), \quad \lambda \ll N, \quad N \gg 1. \tag{9}$$

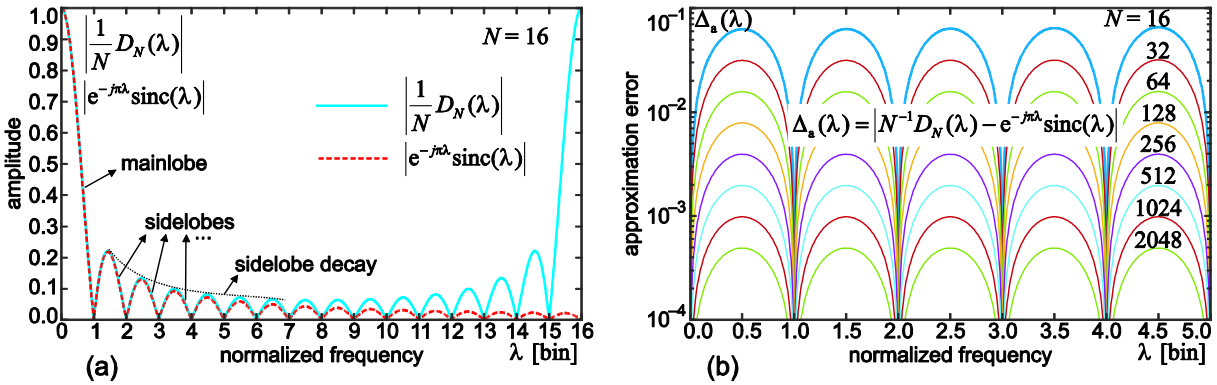

Fig. 1. Frequency amplitude characteristic $D_N(\lambda)$ of the rectangular window defined by (8) and its approximation defined by (9): (a) example for $N = 16$; (b) approximation error Δ_a for $\lambda < 5$ and various N – the error halves with each doubling of N.

The sinc(λ) function appearing in (9) is commonly known as the "decaying sinusoid" function, with an amplitude envelope that behaves according to the hyperbolic function λ^{-1}. The graph of $D_N(\lambda)$ or $|\text{sinc}(\lambda)|$ for $\lambda \in [-1, 1]$ determines the main lobe of the frequency response with a width of $MLBW = 1$ bin (this is the distance on the frequency axis from the point $\lambda = 0$ to the first zero of the $D_N(\lambda)$ function), and the subsequent periods of the "decaying sinusoid" define the additional side lobes (Fig. 1a). The conditions of approximation (9) mean that the approximation can be used for the main lobe and initial side lobes (condition $\lambda \ll N$) and with a sufficiently large number N of signal samples (Fig. 1b). It is also worth mentioning that approximation (9) removes the periodicity feature from the $D_N(\lambda)$ function defined by (8) (Fig. 1a). When analyzing function (8) across the full range of the spectrum, it is also notable that subsequent periods of this function do not influence the values of this function in the first period, *i.e.* for $0 \le \lambda < N$.

The purpose of using windows other than the rectangular window is to achieve high attenuation of side lobes (thereby limiting the mutual influence of different components in the spectrum), which is achieved at the expense of broadening the main lobe (which degrades the frequency resolution of spectrum analysis) and increasing noise in the spectrum by the so-called *Equivalent Noise Band Width* (*ENBW*) factor [6]. The family of GMSD time windows described later in the paper defines a time window with parameter p, and the ability to adjust this parameter allows for a suitable compromise between high sidelobe attenuation and limited main lobe width and *ENBW* value.

3. GMSD windows – definitions

Windows with maximum sidelobe decay and a parameter $p = 2r + z$ (where $z = 0$ for an even p, $z = 1$ for an odd p and r is a non-negative integer) are defined either by the $\sin^p$:

$$w_n = sin^p\left(\frac{\pi n}{N}\right) = sin^{2r+z}\left(\frac{\pi n}{N}\right), \quad n = 0, \ldots, N-1 \tag{10}$$

or by using appropriate trigonometric series of order $r = H–1$ with the number of a_h coefficients equal to $H = r + 1$:

$$w_n = \sum_{h=0}^{H-1}(-1)^h a_h \cos\left[\frac{(2h+z)\pi n}{N} - \frac{z\pi}{2}\right], \quad p = 2r + z, \quad H = r + 1 \tag{11}$$

or, considering that $\cos(\alpha - \pi/2) = \sin(\alpha)$:

$$w_n = \begin{cases} \sum_{h=0}^{H-1}(-1)^h a_h \cos\frac{2h\pi n}{N} & \text{for } p = 2r \quad (12) \\ \sum_{h=0}^{H-1}(-1)^h a_h \sin\frac{(2h+1)\pi n}{N} & \text{for } p = 2r+1 \quad (13) \end{cases},$$

where the coefficients a_h are defined as (Table 1) [14]:

$$a_0 = \frac{1}{2^{2r}}\binom{p}{r}, \quad a_h = \frac{1}{2^{p-1}}\binom{p}{r-h}, \quad h = 1, \ldots, r, \tag{14}$$

and for a given p:

$$r = \left\lfloor \frac{p}{2} \right\rfloor, \quad H = \left\lfloor \frac{p}{2} \right\rfloor + 1, \quad z = [1 - (-1)^p]/2. \tag{15}$$

The symbol $\lfloor x \rfloor$ denotes the integer part of x, meaning rounding down (floor(x) function), and the binomial coefficient is defined as:

$$\binom{p}{r} = \frac{p!}{r!\,(p-r)!} \tag{16}$$

Table 1. Coefficients a_h for p = 0, …, 13

p	0	1	2	3	4	5	6	7	8	9	10	11	12	13
r	0	0	1	1	2	2	3	3	4	4	5	5	6	6
z	0	1	0	1	0	1	0	1	0	1	0	1	0	1
a_0	1	1	1/2	3/4	3/8	10/16	10/32	35/64	35/128	126/256	126/512	462/1024	462/2048	1716/4096
a_1	–	–	1/2	1/4	4/8	5/16	15/32	21/64	56/128	84/256	210/512	330/1024	792/2048	1287/4096
a_2	–	–	–	–	1/8	1/16	6/32	7/64	28/128	36/256	120/512	165/1024	495/2048	715/4096
a_3	–	–	–	–	–	–	1/32	1/64	8/128	9/256	45/512	55/1024	220/2048	286/4096
a_4	–	–	–	–	–	–	–	–	1/128	1/256	10/512	11/1024	66/2048	78/4096
a_5	–	–	–	–	–	–	–	–	–	–	1/512	1/1024	12/2048	13/4096
a_6	–	–	–	–	–	–	–	–	–	–	–	–	1/2048	1/4096

The equivalence of relations (10) and (12), (13) for a_h defined by (14)–(16) can be demonstrated based on the relations [19]:

$$\sin^{2n} x = \frac{1}{2^{2n}}\left[\sum_{k=0}^{n-1}(-1)^{n-k} 2\binom{2n}{k}\cos 2(n-k)x + \binom{2n}{n}\right], \tag{17}$$

$$\sin^{2n-1} x = \frac{1}{2^{2n-2}}\sum_{k=0}^{n-1}(-1)^{n+k-1}\binom{2n-1}{k}\sin(2n-2k-1)x. \tag{18}$$

By making substitutions in (17): $n \to r$, $k \to (r - h)$, $x \to \pi n/N$, the relation (12) for $p = 2r$ with coefficients a_h defined by (14) is obtained. By making substitutions in (18): $n \to r + 1$, $k \to (r - h)$, $x \to \pi n/N$, the relation (13) for $p = 2r + 1$ with coefficients a_h also defined by (14) is obtained.

The definition (10) of GMSD windows is very convenient for the use in signal analysis because it contains only one parameter p. However, to demonstrate certain properties of these windows, the form (11) or (12), (13) is more suitable, so these definitions will be used in the subsequent sections.

4. GMSD windows for even *p*: A review

Windows defined by (12) were first analyzed extensively in terms of selecting a_h coefficients that ensure maximum sidelobe amplitude decay by Rife and Vincent [1]. Presented here is a summary of the key stages of Rife and Vincent's analysis supplemented by findings from [12], which collectively demonstrate that the a_h coefficients defined by (14) ensure maximum sidelobe amplitude decay for the given value H and also meet the normalization condition $\max_n w_n = 1$.

From (7), (8), and (12), the DtFT of such windows has the following form:

$$W(\lambda) = \sum_{h=0}^{H-1}(-1)^h \frac{a_h}{2}[D_N(\lambda - h) + D_N(\lambda + h)]. \tag{19}$$

Taking into account (19), approximation (9) and the relation

$$sin(\pi(\lambda + k)) = (-1)^k sin(\pi\lambda), \quad k = 0, \pm1, \pm2, \ldots, \tag{20}$$

the following is obtained [1]:

$$W(\lambda) = \frac{N}{\pi}\lambda\, sin(\pi\lambda) e^{-j\pi\lambda} \sum_{h=0}^{H-1}(-1)^h \frac{a_h}{\lambda^2 - h^2}. \tag{21}$$

The components of series (21) can be written with a common denominator [1]:

$$W(\lambda) = N e^{-j\pi\lambda} \frac{sin(\pi\lambda)}{\pi\lambda} \frac{P(\lambda)}{\prod_{h=1}^{H-1}(\lambda^2 - h^2)}, \tag{22}$$

where $P(\lambda)$ is a polynomial of variable λ [1]:

$$P(\lambda) = \lambda^2[\prod_{h=1}^{H-1}(\lambda^2 - h^2)] \cdot \left[\sum_{h=0}^{H-1}(-1)^h \frac{a_h}{\lambda^2 - h^2}\right] = \sum_{h=0}^{H-1}\left[(-1)^h a_h \prod_{k=0, k\neq h}^{H-1}(\lambda^2 - k^2)\right]. \tag{23}$$

For integer values of λ, the following is obtained [1]:

$$P(h) = (-1)^h a_h \prod_{k=0, k\neq h}^{H-1}(h^2 - k^2), \text{ for } h = 0, 1, \ldots, H-1. \tag{24}$$

Rife and Vincent demonstrated in [1] that $P(\lambda)$ should be constant, *i.e.* $P(\lambda) = P(0)$, to obtain maximum sidelobe decay in (22) with an increase of λ. From this fact and (24),

$$(-1)^h a_h \prod_{k=0, k\neq h}^{H-1}(h^2 - k^2) = a_0 \prod_{k=1}^{H-1}(-k^2), \text{ for } h = 0, 1, \ldots, H-1, \tag{25}$$

and after some transformations, the following is obtained [1]:

$$a_h = 2a_0 \frac{[(H-1)!]^2}{(H-1-h)!(H-1+h)!} = 2a_0 \prod_{k=0}^{h-1} \frac{H-h+k}{H+k}, \; h \geq 1. \tag{26}$$

The relation (26) can be written with the use of Newton's binomial symbol [12]:

$$a_h = 2a_0 \binom{2(H-1)}{H-1}^{-1} \binom{2(H-1)}{H-1-h}, \quad h \geq 1. \tag{27}$$

Based on (27) and the property of Newton's binomial

$$\sum_{k=0}^{r}\binom{2r}{k} = 2^{2r-1} + \frac{1}{2}\binom{2r}{r}, \tag{28}$$

the following is obtained:

$$\sum_{h=0}^{H-1} a_h = a_0 2^{2(H-1)} \binom{2(H-1)}{H-1}^{-1}. \tag{29}$$

It is possible to assume, as in [1], that a_0 equals 1 or any other constant, which is equivalent to multiplying the obtained spectrum by this constant. For time windows, the normalization condition $\max_n w_n = 1$ is usually assumed, which means that $w_{N/2} = 1$ due to the window

symmetry. From this fact applied to (12), it follows that the sum (29) must be equal to 1, so based on (27) and (29), the final dependencies for a_h are obtained as (14).

The above derivation of a_h directly from the Rife and Vincent result (26) was briefly presented in [12]. In [7] the author obtained this form of a_h through induction and proved that three necessary conditions are fulfilled: sum (29) equals 1 and the following additional relations obtained by Nuttall in [3]:

$$\sum_{h=0}^{H-1}(-1)^h a_h = 0, \tag{30}$$

$$\sum_{h=0}^{H-1}(-1)^h h^{2m} a_h = 0,\ m \geq 1. \tag{31}$$

The spectrum of time windows (12) with coefficients defined by (14) is obtained from (22), (24), (14) and $P(\lambda) = P(0)$ (some variations of this relation can be found in [1], [3], [9], [7], [10], [11]):

$$W(\lambda) = \frac{N}{2^{2H-2}} \frac{\sin(\pi\lambda)}{\pi\lambda} e^{-„j\pi" \lambda} \frac{(2H-2)!}{\prod_{h=1}^{H-1}(h^2-\lambda^2)}. \tag{32}$$

5. GMSD windows for odd *p*

Proof that the coefficients defined in (14) ensure maximum sidelobe amplitude decay condition for windows defined by (13), for the given value *H*, is published below for the first time, although the general method of its execution was already mentioned in [14].

As in (19) for the windows defined by (12), the DtFT of the windows defined by (13) has the following form:

$$W(\lambda) = \sum_{h=0}^{H-1}(-1)^h \frac{a_h}{2j}\left[D_N\left(\lambda - (h+\frac{1}{2})\right) - D_N\left(\lambda + (h+\frac{1}{2})\right)\right]. \tag{33}$$

Taking into account (9), relation (33) has the following form:

$$W(\lambda) = -\frac{N}{\pi} cos(\pi\lambda) e^{-\mathrm{j}\pi\lambda} \sum_{h=0}^{H-1}(-1)^h a_h \frac{h+\frac{1}{2}}{\lambda^2-(h+\frac{1}{2})^2}. \tag{34}$$

The components of series (34) can be written with a common denominator

$$W(\lambda) = -\frac{N}{\pi} cos(\pi\lambda) e^{-\mathrm{j}\pi\lambda} \frac{P(\lambda)}{\prod_{h=0}^{H-1}\left[\lambda^2-(h+\frac{1}{2})^2\right]}, \tag{35}$$

where $P(\lambda)$ is a polynomial of variable λ:

$$\begin{aligned} P(\lambda) &= \left[\prod_{h=0}^{H-1}\left[\lambda^2 - \left(h+\frac{1}{2}\right)^2\right]\right] \cdot \left[\sum_{h=0}^{H-1}(-1)^h a_h \frac{h+\frac{1}{2}}{\lambda^2-\left(h+\frac{1}{2}\right)^2}\right] \\ &= \sum_{h=0}^{H-1}(-1)^h a_h (h+\tfrac{1}{2}) \prod_{k=0,\ k\neq h}^{H-1}[\lambda^2 - (k+\tfrac{1}{2})^2]. \end{aligned} \tag{36}$$

For $\lambda = h + 1/2$, the following is obtained:

$$\begin{aligned} P(h+\tfrac{1}{2}) &= (-1)^h a_h (h+\tfrac{1}{2}) \prod_{k=0,k\neq h}^{H-1}[(h+\tfrac{1}{2})^2 - (k+\tfrac{1}{2})^2] \\ &= (-1)^h a_h (h+\tfrac{1}{2}) \prod_{k=0,\ k\neq h}^{H-1}(h-k)(h+k+1), \quad h = 0,1,\ldots,H-1. \end{aligned} \tag{37}$$

The polynomial $P(\lambda)$ should be constant, *i.e.* $P(h+1/2) = P(0+1/2)$, to obtain the maximum sidelobe decay in (35) with an increase of λ. From this fact and (37):

$$(-1)^h a_h (h+\tfrac{1}{2}) \prod_{k=0,k\neq h}^{H-1}(h-k)(h+k+1) = a_0 \frac{1}{2} \prod_{k=1}^{H-1}(-k)(k+1), \tag{38}$$

and after some transformations, the following is obtained:

$$a_h = a_0 \binom{2(H-1)+1}{(H-1)}^{-1} \binom{2(H-1)+1}{(H-1)-h}. \tag{39}$$

Based on (39) and the property of Newton's binomial:

$$\sum_{k=0}^{r} \binom{2r+1}{k} = 2^{2r}, \tag{40}$$

the following is obtained:

$$\sum_{h=0}^{H-1} a_h = a_0 2^{2(H-1)} \binom{2H-1}{H-1}^{-1}. \tag{41}$$

For the normalization condition $\max_n w_n = 1$, *i.e.* $w_{N/2} = 1$ due to the window symmetry, and from (13), it follows that sum (41) must be equal to 1, so based on (39) and (41), the final dependencies (14) for a_h are obtained.

The spectrum of time windows (13) with coefficients defined by (14) is obtained from (35) for $P(\lambda) = P(1/2)$ (because $P(\lambda)$ is constant), (37) for $h = 0$, and (14) [14]:

$$W(\lambda) = \frac{N}{\pi 2^{2H-1}} \cos(\pi\lambda)\, e^{-„j\pi" \lambda} \frac{(2H-1)!}{\prod_{h=0}^{H-1}\left[\left(h+\frac{1}{2}\right)^2 - \lambda^2\right]}. \tag{42}$$

6. Analytical form of the spectrum of GMSD windows

Based on (32) for even p, (42) for odd p and (15) the spectrum of GMSD windows defined by (10) for any p is given by [14]:

$$W_p(\lambda) = \frac{D_p(\lambda)}{P_p(\lambda)}, \tag{43}$$

where [14]:

$$D_p(\lambda) = \frac{N}{\pi} \frac{p!}{2^p} e^{-\mathrm{j}\pi\lambda} \sin(\pi\lambda + z\pi/2), \tag{44}$$

$$P_p(\lambda) = (-1)^{(r+z)} \lambda^{z-1} \prod_{h=0}^{r} [\lambda^2 - (h + z/2)^2] = (-1)^{(r+z)} \prod_{h=-(r+z)}^{r} (\lambda + h + z/2) \tag{45}$$

Based on the above equations, the following is obtained for natural numbers n [14]:

$$D_p(\lambda + n) = D_p(\lambda), \tag{46}$$

$$P_p(\lambda + n) = P_p(\lambda) \prod_{m=1}^{n} \frac{2(\lambda+m)+p}{2(\lambda+m-1)-p}, \tag{47}$$

and then [14]:

$$W_p(\lambda + n) = W_p(\lambda) \prod_{m=1}^{n} \frac{2(\lambda+m-1)-p}{2(\lambda+m)+p}. \tag{48}$$

From (44) and (45), the following properties also arise

$$(p+1) D_p(\lambda) = 2(-1)^p e^{-j\pi/2} D_{p+1}(\lambda + \tfrac{1}{2}), \tag{49}$$

$$[2(\lambda+1)+p] P_p(\lambda) = 2(-1)^{p+1} P_{p+1}(\lambda + \tfrac{1}{2}), \tag{50}$$

which after n-fold recursion leads to:

$$D_p(\lambda) \prod_{m=1}^{n} (p+m) = 2^n (-1)^{np+n(n-1)/2} e^{-j\pi n/2} D_{p+n}(\lambda + n/2), \tag{51}$$

$$P_p(\lambda) \prod_{m=1}^{n} [2(\lambda+m)+p] = 2^n (-1)^{np+\frac{n(n+1)}{2}} P_{p+n}\left(\lambda + \frac{n}{2}\right). \tag{52}$$

Equations (51), (52) can be proved by mathematical induction on n. For $n = 1$ (51), (52) are true due to (49), (50). By the assumption that (51), (52) are true for $n > 1$, it follows from (49), (50) that they are true for $n + 1$. This means, based on mathematical induction, that (51), (52) are true for any natural n.

From (43), (51), (52):

$$W_p(\lambda) = e^{"j\pi"\frac{n}{2}} W_{p+n}\left(\lambda + \frac{n}{2}\right) \prod_{m=1}^{n} \frac{2(\lambda+m)+p}{p+m}, \tag{53}$$

$$W_{p+n}\left(\lambda + \frac{n}{2}\right) = e^{-"j\pi"\frac{n}{2}} W_p(\lambda) \prod_{m=1}^{n} \frac{p+m}{2(\lambda+m)+p}. \tag{54}$$

From the quotient of (48) for $n = k$ and (54) for $n \geq k$ the following is obtained:

$$W_p(\lambda + k) = W_{p+n}(\lambda + n/2) \cdot e^{j\pi n/2} \frac{\prod_{m=1}^{k}[2(\lambda+m-1)-p] \prod_{m=k+1}^{n}[2(\lambda+m)+p]}{\prod_{m=1}^{n}(p+m)}. \tag{55}$$

Here, the following notation is assumed

$$\prod_{m=n_1}^{n_2}[\cdot] = 1, \quad \text{for} \quad n_2 < n_1, \tag{56}$$

which appears in (55) in the numerator when $n = k$.

7. Selected properties of GMSD windows

Time and frequency characteristics of GMSD windows for values $p = 0, 1, \ldots, 11$ for form (10) are presented in Fig. 2.

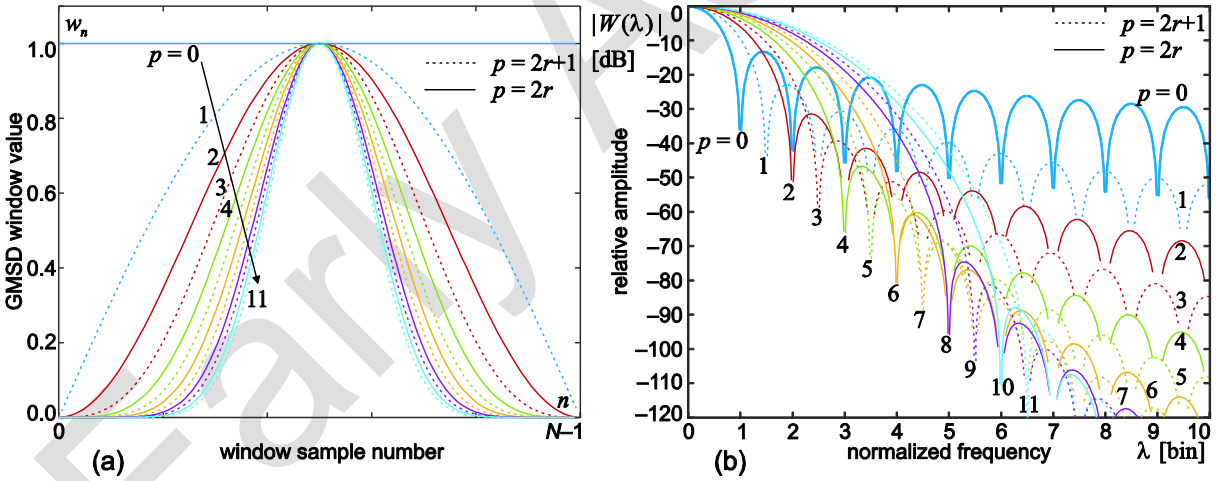

Fig. 2. GMSD data windows: (a) time characteristics, (b) frequency amplitude characteristics.

The main lobe width (*MLBW*) for GMSD windows is:

$$MLBW = 1 + \frac{p}{2} \text{ [bin]}. \tag{57}$$

The asymptotic sidelobe amplitude decay of GMSD windows is equal $6(p + 1)$ dB/oct.

The most important parameter of a data window that defines its statistical properties is the *Equivalent Noise Band Width* (*ENBW*) coefficient, which is the ratio of Normalized Noise Power Gain (*NNPG*) to the square of *Normalized Peak Signal Gain* (*NPSG*) [6]:

$$ENBW = \frac{NNPG}{(NPSG)^2} = N \frac{\left(\sum_{n=0}^{N-1} w_n^2\right)}{\left(\sum_{n=0}^{N-1} w_n\right)^2}, \tag{58}$$

where $NNPG = \frac{1}{N}\sum_{n=0}^{N-1} w_n^2$ and $NPSG = \frac{1}{N}\sum_{n=0}^{N-1} w_n$.

The analytical calculation of the *NNPG*, *NPSG* and *ENBW* values is possible by using the following relation:

$$\sum_{n=0}^{N-1} sin^p \frac{\pi n}{N} = \begin{cases} Na_0 & \text{for } p = 2r \\ \sum_{h=0}^{r} (-1)^h a_h \, cot \frac{(2h+1)\pi}{2N} & \text{for } p = 2r+1 \end{cases}. \tag{59}$$

For MSD windows, *i.e.* for $p = 2r$, analytical forms of *NNPG*, *NPSG* and then *ENBW* were derived in [7], [11] as a function of a_h coefficients. Combining these relations with (14) allows obtaining an exact relation for *ENBW* in terms of the parameter *p*, albeit using Newton's binomial. This formula, however, does not allow (without additional numerical calculations) to immediately assess the nature of the *ENBW* versus *p* relation (*e.g.*, whether it is linear, square, square root, or other depending on the parameter *p*). This issue is exacerbated for the case $p = 2r + 1$, where (59), in conjunction with (14), reveals substantial differences in the complexity of the analytical relations compared to $p = 2r$ case. Therefore, to obtain an approximate, yet sufficiently accurate and interpretable, analytical expression for *ENBW* as a function of *p* for both cases, the following transformations are presented.

Considering (59) for $p = 2r$ the following is obtained based on (58):

$$ENBW = \binom{2p}{p} \cdot \binom{p}{r}^{-2} \text{ for } p = 2r, \tag{60}$$

resulting in the following exemplary values of *ENBW*: 1 for $p = 0$, 1.5 for $p = 2$, 1.944 for $p = 4$, 2.31 for $p = 6$, 2.627 for $p = 8$ and 2.909 for $p = 10$.

To simplify (60), Stirling's approximation [20] can be used:

$$n! \cong \sqrt{2\pi n}\left(\frac{n}{e}\right)^n. \tag{61}$$

Using (61) in relation (60) yields:

$$ENBW \cong \sqrt{\frac{\pi}{4}p}. \tag{62}$$

Stirling's formula (61) is usually applied for large values of *n* when calculating *n*! (for $n = 0$ it even gives an incorrect result). Since *p* typically takes on small values in practice, the relation (61) is used here only for a qualitative assessment of the *ENBW* dependency on the parameter *p*. It allows for the assumption that the square of the *ENBW* coefficient for a GMSD window with parameter *p* is approximately a linear function of *p*. After applying linear regression to the square of *ENBW* as a function of *p* for the most practical range $p = 1, \ldots, 11$ the following is obtained [21]:

$$ENBW(p) \cong \begin{cases} 1 & \text{for } p = 0 \\ \sqrt{a \cdot p + b}, \; a = 0.78, b = 0.70 & \text{for } p = 1, \; \ldots, \; 11 \end{cases}. \tag{63}$$

Applying the least squares fitting method to obtain (63) means that it can be used for all values of the parameter *p* (Fig. 3), not just for even *p*, as assumed in (60). For $p > 11$ the values of *a* and *b* may change slightly.

To account for the case of $p = 0$ a modification of Stirling's formula proposed by Gosper [20] can be used in the approximation, where instead of the standard term $\sqrt{2\pi n}$, an adjustment $\sqrt{(2\pi n + \pi/3)}$ is utilized, and the approximation $\sqrt{\pi/3} = 1.023\ldots \approx 1$ is employed, which allows for the approximation to be applied for $n = 0$ (0! = 1). In this way, a

single relation is obtained for all p ≥ 0 (Fig. 3):

$$ENBW(p) \cong \frac{1}{2} \cdot \frac{(p+1/3)^2}{(p+1/6)^2} \sqrt{\pi(p+1/12)} \cong \frac{1}{2} \cdot \frac{(p+1/3)^2}{(p+1/6)^2} \sqrt{\pi p + 1/4}. \quad (64)$$

The values of *ENBW* coefficient for GMSD windows defined by (58) and approximated by (63) or (64) practically do not depend on *N* (for *N* equal 32 or greater). The reciprocal of *ENBW* coefficient is called in [2] as a *Processing Gain* (*PG*) coefficient. Applying data window with coefficient *ENBW* higher than one implies that the so-called noise-floor in the spectrum has higher values (is multiplied by *ENBW* value) [4]–[6].

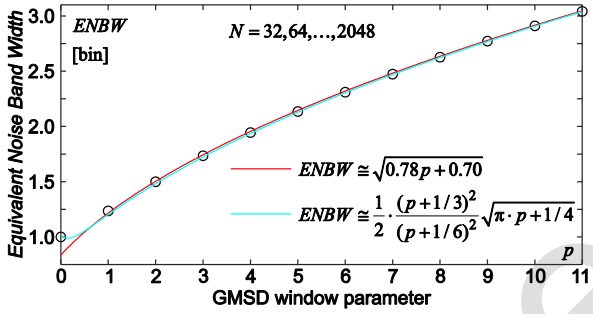

Fig. 3. Coefficient *ENBW* of GMSD windows as a function of parameter *p*: calculated based on (58) for natural *p* (circle centres) and its approximation by (63) and (64). The approximation error is within the range [–0.01, +0.01] bin, except for case (63) for *p* = 1 (with the error ca. –0.02 bin) and case (64) for 0 ≤ *p* ≤ 3 (with the error in the range [–0.033, +0.023] bin).

8. Conclusions

The paper summarizes the most important properties (both previously known and new ones) of power-of-sine windows, also referred to ([14], [16], [21]) as *Generalized Maximum Sidelobe Decay* (GMSD) windows. The term GMSD for power-of-sine windows is justified by the following two facts (Sec. 3-5):

– GMSD windows include as a subfamily (for even *p*) *Maximum Sidelobe Decay* (MSD) windows,
– GMSD windows exhibit the property of maximum sidelobe decay for all integer values of *p* > 0 (both even and odd) for a given number *H* of coefficients in the trigonometric series expansion (11).

Using only one parameter *p* (instead of a set of a_h coefficients as is the case for MSD windows) is particularly convenient when using the window for computing the spectrum of a measured signal. For the same reason, in Sec. 6-7, a number of formulas defining the properties of the frequency characteristics of GMSD windows and their selected coefficients (*MLBW*, *ENBW*) as a function of parameter *p* are presented. A well-defined frequency characteristic of GMSD windows given by (43)-(45) has already been applied in the development of new spectrum interpolation methods (IpDFT) [14], [16]. Other relations presented in Sec. 6-7 may be helpful further in new applications of GMSD windows.

The primary contributions of this paper are the rigorous proof of the maximum sidelobe decay property for *p* = 2*r* + 1 (Sec. 5), as well as the derivation of several novel relations in Sec. 6 and 7, particularly concerning the frequency characteristic and *ENBW* coefficient as a function of the parameter *p*.

References

[1] Rife, D. C., & Vincent, G. A. (1970). Use of the Discrete Fourier Transform in the Measurement of Frequencies and Levels of Tones. *Bell System Technical Journal*, *49*(2), 197–228. https://doi.org/10.1002/j.1538-7305.1970.tb01766.x

[2] Harris, F. J. (1978). On the use of windows for harmonic analysis with the discrete Fourier transform. *Proceedings of the IEEE*, *66*(1), 51–83. https://doi.org/10.1109/proc.1978.10837

[3] Nuttall, A. (1981). Some windows with very good sidelobe behavior. *IEEE Transactions on Acoustics, Speech, and Signal Processing*, *29*(1), 84–91. https://doi.org/10.1109/tassp.1981.1163506

[4] Offelli, C., & Petri, D. (1991). Weighting effect on the discrete time Fourier transform of noisy signals. *IEEE Transactions on Instrumentation and Measurement*, *40*(6), 972–981. https://doi.org/10.1109/19.119777

[5] Offelli, C., & Petri, D. (1992). The influence of windowing on the accuracy of multifrequency signal parameter estimation. *IEEE Transactions on Instrumentation and Measurement*, *41*(2), 256–261. https://doi.org/10.1109/19.137357

[6] Solomon, O. M. (1992). The effects of windowing and quantization error on the amplitude of frequency-domain functions. *IEEE Transactions on Instrumentation and Measurement*, *41*(6), 932–937. https://doi.org/10.1109/19.199437

[7] Belega, D. (2005). The maximum sidelobe decay windows. *Revue Roumaine des Sciences Techniques. Série Electrotechnique et Energetique*, *50*(3), 349–356.

[8] Zivanovic, M., & Carlosena, A. (2001). Nonparametric spectrum interpolation methods: a comparative study. *IEEE Transactions on Instrumentation and Measurement*, *50*(5), 1127–1132. https://doi.org/10.1109/19.963171

[9] Agrež, D. (2002). Weighted multipoint interpolated DFT to improve amplitude estimation of multifrequency signal. *IEEE Transactions on Instrumentation and Measurement*, *51*(2), 287–292. https://doi.org/10.1109/19.997826

[10] Belega, D., & Dallet, D. (2008). Frequency estimation via weighted multipoint interpolated DFT. *IET Science, Measurement & Technology*, *2*(1), 1–8. https://doi.org/10.1049/iet-smt:20070022

[11] Belega, D., & Dallet, D. (2009). Multifrequency signal analysis by interpolated DFT method with maximum sidelobe decay windows. *Measurement*, *42*(3), 420–426. https://doi.org/10.1016/j.measurement.2008.08.006

[12] Borkowski, J., Kania, D., & Mroczka, J. (2014). Interpolated-DFT-Based Fast and Accurate Frequency Estimation for the Control of Power. *IEEE Transactions on Industrial Electronics*, *61*(12), 7026-7034. https://doi.org/10.1109/TIE.2014.2316225

[13] Duda, K., & Barczentewicz, S. (2014). Interpolated DFT for $\sin^{\alpha}(x)$ Windows. *IEEE Transactions on Instrumentation and Measurement*, *63*(4), 754–760. https://doi.org/10.1109/TIM.2013.2285795

[14] Borkowski, J., Mroczka, J., Matusiak, A., & Kania, D. (2021). Frequency Estimation in Interpolated Discrete Fourier Transform with Generalized Maximum Sidelobe Decay Windows for the Control of Power. *IEEE Transactions on Industrial Informatics*, *17*(3), 1614–1624. https://doi.org/10.1109/TII.2020.2998096

[15] Wang, K., Wen, H., & Li, G. (2021). Accurate Frequency Estimation by Using Three-Point Interpolated Discrete Fourier Transform Based on Rectangular Window. *IEEE Transactions on Industrial Informatics*, *17*(1), 73–81. https://doi.org/10.1109/TII.2020.2981542

[16] Matusiak, A., Borkowski, J., & Mroczka, J. (2022). Noniterative method for frequency estimation based on interpolated DFT with low-order harmonics elimination. *Measurement*, *196*(111241), 1–9. https://doi.org/10.1016/j.measurement.2022.111241

[17] Rodrigues, N. M., Janeiro, F. M., & Ramos, P. M. (2022). Implementation of Goertzel-based frequency estimation for power quality monitoring in embedded measurement systems. *Metrology and Measurement Systems*, *29*(3), 455–468. https://doi.org/10.24425/mms.2022.142270

[18] Zhang, J., Song, J., Li, C., Xu, X., & Wen, H. (2024). Novel Frequency Estimator for Distorted Power System Signals Using Two-Point Iterative Windowed DFT. *IEEE Transactions on Industrial Electronics*, *71*(10), 13372–13383. https://doi.org/10.1109/tie.2023.3347846

[19] Zwillinger, D., Moll, V., Gradshteyn, I. S., & Ryzhik, I. M. (2014). *Table of Integrals, Series, and Products* (Eighth Edition), Academic Press, UK.

[20] Swendsen, R. (2020). *An Introduction to Statistical Mechanics and Thermodynamics* (Second Edition), Oxford University Press, USA.

[21] Borkowski, J., & Mroczka, J. (2019). Influence of Noise on the Interpolated DFT-based Frequency Estimation for the Control of Power Using Generalized Maximum Sidelobe Decay Windows, *42nd International Conference on Telecommunications and Signal Processing, TSP 2019*, 8769023, 269–272. https://doi.org/10.1109/TSP.2019.8769023

Józef Borkowski is a Professor, he received a Ph.D. degree in 1997 and a D.Sc. degree in 2012 in the field of Electronics. He is currently a Professor at Wroclaw University of Science and Technology, within the Chair of Electronic and Photonic Metrology. His main research areas are: precise spectrum analysis methods (IpDFT, LIDFT), image analysis (geometric matching of circular elements), data processing in measurements using DSP methods, and methods of analysis and data processing in renewable energy systems.

Adam Matusiak obtained the M.Sc. and Ph.D. degree in electronics from the Wroclaw University of Science and Technology, Poland, in 2017 and 2024 respectively. He is currently Assistant Professor at the same university, within the Chair of Electronic and Photonic Metrology. His current research interests include signal processing and its integration with real-time measurement systems